THE JOURNAL OF BIOLOGICAL CHEMISTRY VOL. 287, NO. 50, pp. 42288–42298, December 7, 2012

Hyaluronan and Layilin Mediate Loss of Airway Epithelial Barrier Function Induced by Cigarette Smoke by Decreasing E-cadherin*[S]

Received for publication, June 1, 2012, and in revised form, September 20, 2012 Published, JBC Papers in Press, October 9, 2012, DOI 10.1074/jbc.M112.387795

Rosanna Malbran Forteza[‡], S. Marina Casalino-Matsuda[§], Nieves S. Falcon[‡], Monica Valencia Gattas[¶], and Maria E. Monzon[‡1]

From the [‡]Division of Pulmonary Critical Care, Sleep and Allergy Medicine, [¶]Department of Cell Biology and Anatomy, University of Miami Miller School of Medicine, Miami, Florida 33136 and the [§]Division of Pulmonary and Critical Care Medicine, Feinberg School of Medicine, Northwestern University, Chicago, Illinois 60611

Background: Cigarette smoke (CigS) induces hyaluronan fragmentation and increases epithelial permeability.
Results: CigS and HA fragments decrease E-cadherin expression that is prevented by knocking down layilin.
Conclusion: HA fragments bind to layilin and signal through RhoA/ROCK to inhibit E-cadherin.
Significance: Airway epithelium is our first line of defense against inhaled insults. HA fragments released by CigS disrupt this barrier.

Cigarette smoke (CigS) exposure is associated with increased bronchial epithelial permeability and impaired barrier function. Primary cultures of normal human bronchial epithelial cells exposed to CigS exhibit decreased E-cadherin expression and reduced transepithelial electrical resistance. These effects were mediated by hyaluronan (HA) because inhibition of its synthesis with 4-methylumbelliferone prevented these effects, and exposure to HA fragments of <70 kDa mimicked these effects. We show that the HA receptor layilin is expressed apically in human airway epithelium and that cells infected with lentivirus expressing layilin siRNAs were protected against increased permeability triggered by both CigS and HA. We identified RhoA/Rho-associated protein kinase (ROCK) as the signaling effectors downstream layilin. We conclude that HA fragments generated by CigS bind to layilin and signal through Rho/ROCK to inhibit the E-cadherin gene and protein expression, leading to a loss of epithelial cell-cell contact. These studies suggest that HA functions as a master switch protecting or disrupting the epithelial barrier in its high *versus* low molecular weight form and that its depolymerization is a first and necessary step triggering the inflammatory response to CigS.

Cigarette smoke (CigS)[2] exposure is a risk factor for the development of chronic obstructive pulmonary disease (COPD) and the exacerbation of asthma (1–4). The airway epithelium together with an adequate mucociliary clearance provide the first line of defense against inhaled noxious insults. The epithelial barrier structure and integrity are maintained by the apical junctional complex (AJC), a highly specialized structure that includes tight junctions and adherens junctions. The AJC is composed of a number of transmembrane proteins such as occludin, claudin, junctional adhesion molecule, and cadherins as well as intracellular components such as the zonula occludens and catenin families. The AJC is physically associated with and regulated by dynamic changes in the actin cytoskeleton (5).

A persistent increase in airway epithelial permeability occurs in smokers and individuals exposed to secondhand smoke (6–10) where the epithelial barrier is disrupted and the subepithelial tissue gets directly exposed to more than 4700 reactive chemicals and 1014 oxidants/free radicals (11, 12). This insult triggers an inflammatory response that, if sustained, can lead to structural epithelial abnormalities such as remodeling and mucous metaplasia (13), both hallmarks of COPD and asthma. The mechanisms responsible for epithelial permeability regulation are quite complex and involve a number of biochemical and cellular pathways/events (14), including the activation of small GTPases of the Rho family (15, 16).

Hyaluronan (HA) is a linear nonsulfated glycosaminoglycan widely distributed in the tissues of all vertebrates (17) that in the airways is synthesized by surface epithelial cells and submucosal glands as a high molecular weight polymer (~2 MDa). It plays a key role in mucosal host defense by retaining and regulating enzymes important for homeostasis, stimulating ciliary

* This work was supported, in whole or in part, by National Institutes of Health Grants HL073156 and HL08992. This work was also supported by grants from the Flight Attendant Medical Research Institute (to M. E. M.), Bridge Award JEK12292 from the James and Esther King Foundation, a Clinical Innovator Award from Flight Attendant Medical Research Institute (to R. M. F.), Scientist Development Grant 635093N from the American Heart Association, and James and Esther King Foundation Grant JEK 07KN-02 12324 1 (to S. M. C. M.).

[S] This article contains supplemental Figs. 1–8.

[1] To whom correspondence should be addressed: Division of Pulmonary, Critical Care, Sleep and Allergy Medicine, University of Miami Miller School of Medicine; 1600 NW 10th Ave., Miami, FL 33136. Fax: 305-243-2992; E-mail: mmonzonmedina@med.miami.edu.

[2] The abbreviations used are: CigS, cigarette smoke; AJC, apical junctional complex; ALI, air-liquid interface; C3, C3 exoenzyme; COPD, chronic obstructive pulmonary disease; CS, chondroitin sulfate; ROCK, Rho-associated protein kinase; NHBE, normal human tracheo-bronchial epithelial; HA, hyaluronan; HAS, hyaluronan synthase; MU, 4-methylumbelliferone; oHA, oligosaccharide of HA; RHAMM, receptor for hyaluronan-mediated motility; RON, recepteur d'origine nantais; siLy, Layilin small interference RNA; TEER, trans-epithelial electrical resistance; NTsi, nontargeting sequence; WB, Western blot; qPCR, quantitative real time PCR.

beating through its interaction with RHAMM, and inducing mucin up-regulation by promoting EGF receptor/CD44 interaction (18–22). Smooth muscle cells exposed to polyinosinic-polycytidylic acid release an abnormal HA matrix with cable-like structures that bind and retain leukocytes, suggesting that HA also plays a role in airway host defense against infections (23). Biological effects of HA are dependent on its size (24), local concentration (25), and its interaction with binding proteins (26). These proteins (hyaladherins) organize HA in the matrix (27, 28) and modulate its interaction with specific receptors (29). It has been reported that low molecular weight HA disrupts barrier function in endothelial cells (30), promotes cell migration in tumor cells (31, 32), and both inhibition and stimulation of HA synthesis can suppress the expression of members of the cadherin family and therefore cell-cell adhesion (33, 34).

HA fragmentation can be achieved by direct action of reactive oxygen species (as the ones present in CigS (35, 36)) and/or hydrolysis/lysis by specific glycosidases (hyaluronidases). We have recently shown that reactive oxygen species and Hyal2 work in concert to regulate airway epithelial hyaluronan fragmentation (37). Others, as well as our group, have reported increased levels of HA oligosaccharides (oHA) in airway secretions after chronic exposure to CigS (37, 38).

Layilin is a cell surface hyaluronan receptor (39, 40) with an extracellular domain that is homologous to the carbohydrate-recognition domain of C-type lectin. It interacts with merlin and radixin, members of the ezrin, radixin, and moesin family. These proteins are key regulators of cytoskeleton-plasma membrane interactions in polarized cells and thus could be involved in maintaining or disrupting intercellular epithelial contact. Layilin biological functions are mostly unknown, but its expression has been identified in mouse lung tissue (40) and in A549 alveolar cell lines (41).

In this work, we tested the hypothesis that HA fragments released from surface epithelium by CigS are responsible, at least in part, for the disruption of the epithelial barrier and increased epithelial permeability observed in smokers. We propose that these effects are mediated by oHA binding to layilin and that layilin signaling ultimately results in inhibition and/or alteration of AJC. To test this hypothesis, we used fully differentiated primary cultures of human tracheo-bronchial epithelial cells (NHBE) grown at the air-liquid interface (ALI) and tracheal tissue sections obtained from lung donors. We found that CigS exposure increases epithelial permeability and decreases the expression of E-cadherin and that these effects are mediated by oHA. We report here that layilin is expressed at the apical pole of airway epithelial cells and that oHA binding to layilin triggers the RhoA/ROCK signaling pathway ultimately resulting in AJC disruption and increased epithelial permeability.

EXPERIMENTAL PROCEDURES

All materials were purchased from Sigma unless otherwise specified.

Cell cultures of human tracheo-bronchial epithelial (NHBE) cells grown at air-liquid interface (ALI) were prepared as reported previously (42). Human tracheas and main bronchi from donor lungs were obtained through the University of Miami Life Alliance Organ Recovery Agency with approval from the local Institutional Review Board. NHBE cells were obtained by dissecting mucosa from the underlying cartilage. After incubation in 0.05% protease type XIV in DMEM overnight at 4 °C, epithelial cells were released by vigorous shaking and harvested by centrifugation. These cells (P0) were plated on collagen type 1-coated plastic dishes and grown to confluence in bronchial epithelial growth medium yielding undifferentiated airway epithelial cells. Cells were trypsinized (43) and plated (P1) in 12- or 24-mm Transwell clear culture inserts (Corning Costar Corp., Lowell, MA) coated with human placental collagen (42). Cells were grown in a humidified incubator at 37 °C in ambient air supplemented with 5% CO_2, and as soon confluence was reached, apical surfaces were exposed to air until fully re-differentiated (~21 days). Full differentiation was evidenced by the presence of beating cilia and mucus in the apical surface and a resistivity of >700 ohms/cm^2.

Cigarette Smoke Exposure

CigS was generated using a VITROCELL® VC 10® Smoking Robot. The equipment delivers mainstream and sidestream CigS to the connected CULTEX® exposure module housing transwell inserts where cultures were exposed to CigS (44). This system accurately and effectively mimics real life CigS exposure; in this work, cells were exposed to one K3R4F cigarette with a 50-ml puff volume, 2 s duration, and 1 puff/min. This dose was chosen because it was sufficient to induce cell responses without compromising cell viability (supplemental Fig. 1).

Treatments

For air/cigarette smoke exposure, the apical surface of cultures was washed with PBS (with Ca^{2+} and Mg^{2+}), and media were replaced 24 h before experiments. In the experiments aimed at testing the role of HA in CigS-induced epithelial barrier disruption, HA synthesis was inhibited with 4-methylumbelliferone (MU, 1 mM), added to ALI media 48 h before CigS exposure. This dose reduces new synthesis of HA in these cells by ~85% (19) without harmful or cytotoxic effects (supplemental Fig. 2). In HA exposure studies, dose- and size-response curves were obtained by exposing cells to HA (24 h, 10, 50 and 100 μg/ml) of 2.8, 6.5, 35, 70, 132, 866, and 1000 kDa (R&D Systems, Minneapolis, MN, and Hyalose, Oklahoma City, OK), and an effective dose of 50 μg/ml (supplemental Fig. 3, *A* and *B*) and a size of 6.5 kDa was chosen for the experiments. To confirm that the effects observed were indeed due to oHA, we added increasing concentrations of high molecular weight HA (1 MDa, hyalose) and found that adding 50 μg of high molecular weight HA was sufficient to partially block the effects induced by 50 μg of 6.5 kDa of HA and that increasing the ratio of high molecular weight HA/oHA by exposing cells to oHA could be prevented by using an excess of 1 MDa of HA (supplemental Fig. 3*C*). To ensure that the observed effects were not due to contaminants present in HA preparations (*i.e.* lipopolysaccharide), HA digested with *Streptomyces* hyaluronidase, Seikagaku, Tokyo, Japan) was used as an additional control (supplemental Fig. 4). To evaluate RhoA/ROCK signaling, cultures were

treated with the RhoA inhibitor C3 exoenzyme (Cytoskeleton, Inc., Denver, CO; 1 μg/ml) or ROCK inhibitor Y27632 (5 μg/ml) 10 min before exposure to oHA. After treatments, four sets of replicates were used for the following assessments: 1) trans-epithelial electrical resistance (TEER); 2) paracellular transport of fluorescent dextran; 3) E-cadherin gene expression (qPCR); 4) E-cadherin protein expression by immunofluorescence and WB as described below.

Analysis of Epithelial Integrity

TEER was measured using EVOM and Endohm chambers (World Precision Instruments, Sarasota, FL). Paracellular flux was assessed as described by Cereijido *et al.* (45). Briefly, cells were equilibrated for 1 h with P buffer (145 mM NaCl, 10 mM HEPES, pH 7.4, 1.0 mM sodium pyruvate, 10 mM glucose, 3.0 mM $CaCl_2$) on the basal compartment. Alexa 546-dextran (10 kDa, 2 μg/ml, Invitrogen) was added to P buffer, and its appearance at the apical surface was measured after 2 h of incubation at 37 °C. The apical surface was washed with 0.25 ml of P buffer, and unidirectional paracellular movement was calculated by dividing the dextran concentration (fluorescence) of a given sample on the basolateral compartment with the concentration on the apical washes with the appropriate dilution. Fluorescence was quantified using a SpectraMax GeminiEM plate reader (Molecular Devices, LLC, Sunnyvale, CA), and results were expressed as a percentage of fluorescence diffusion (% DFD) compared with diffusion across empty filters (no cells).

Immunofluorescence

Cell Cultures—To evaluate the effect of CigS and oHA on AJC architecture, immunostaining was performed as described elsewhere. Cell layers were treated with 0.2% Triton X-100 in 100 mM KCl, 3 mM $MgCl_2$, 1 mM $CaCl_2$, 200 mM sucrose, and 10 mM HEPES, pH 7.1. After fixation in 3% paraformaldehyde, cells were blocked in 5% milk in PBS and incubated with mouse anti-E-cadherin antibodies (5 μg/ml, Invitrogen) overnight at 4 °C. To localize RhoA and ROCK, cultures were fixed with paraformaldehyde, permeabilized, blocked with BSA 1% in PBS followed by rabbit anti-RhoA, and mouse anti-ROCK-1 (both 4 μg/ml, Santa Cruz Biotechnology) in blocking solution. Specific labeling was detected using Alexa-conjugated secondary antibodies (Invitrogen). F-actin was labeled with phalloidin tagged with Alexa 488, and nuclei were visualized with 4′,6-diamidine-2-phenylindole (DAPI, both from Invitrogen). Corresponding nonimmune IgGs (mouse or rabbit) were used as controls. Membrane supports were removed from inserts and mounted with FLUORO-GEL (EMS, Hatfield, PA) onto glass slides, and images were obtained using a confocal laser scanning microscope Zeiss LSM700 or the Axiovert 200 M fluorescent microscope (Carl Zeiss Meditec, Jena, Germany).

Tracheal Tissue Sections—Paraffin-embedded sections were hydrated and subjected to heat-induced antigen retrieval with 2 mM EDTA, pH 8.0, for 15 min at 100 °C, treated with acetone at 20 °C for 10 min, and blocked with Image-iT® FX (Signal Enhancer, Invitrogen) following the manufacturer's instructions. Immunolocalization was performed as described above under "Cell Cultures."

Morphometry

Epithelial barrier integrity was assessed by immunofluorescence. Images were obtained as described above, and changes in AJC integrity were assessed by the mean linear (Lm) intercept method (46). Briefly, the number of intercepts visualized as E-cadherin immunofluorescent strands were counted along lines drawn in different directions crossing the junctional axis at various *xy* planes where nuclei were visible, ensuring a horizontal cut through the monolayer (20 lines per layer in at least three slides of cells obtained from three different lung donors, from each experimental condition). Results are expressed as Lm ± S.E. of the number of intercepts per 100 μm.

Quantitative Real Time PCR

cDNA samples were obtained after RNA extraction using TRIzol (Invitrogen) and reverse-transcribed using qScript™ cDNA synthesis kit (Quanta Bioscience, Gaithersburg, MD). A premade TaqMan® Gene Expression Assay with TaqMan® MGB probes and FAM™-labeled E-cadherin (Hs00170423_m1), layilin (Hs01595339_m1), HAS2 (Hs00193435_m1), HAS3 (Hs00193436_m1), CD44 (Hs00153304_m1), and RHAMM (Hs00234864_m1) were used to determine gene expression. Reactions were carried out using ICycler IQ apparatus (Bio-Rad); results were normalized using GAPDH (Hs99999905_m1); relative gene expression was determined using the comparative *CT* method (ΔΔ*CT*) (47) and expressed as fold change.

Hyaluronan Size Estimation

To confirm that *in vitro* CigS exposure results in HA fragmentation as observed in smokers (37) and in NHBE cells exposed to reactive oxygen species (18, 48), apical washes were collected, pooled, and digested with proteinase K (125 μg/ml for 2 h at 60 °C) and chondroitinase ABC (0.5 IU/ml) at pH 7.5 where hyaluronidase activity is negligible (49). Digested samples containing equal amounts of HA (1.5 μg) were precipitated in 85% ethanol, resuspended in water, and run in 0.7% agarose Tris acetate/EDTA gels as described (50). HA standards (Select-HA HiLadder and LoLadder, Hyalose) were used to estimate molecular size. An additional gel was run in 1.5% agarose to expand the low molecular size range and treated with hyaluronidase from *Streptomyces* hyalurolyticus (Seikagaku) to confirm that the observed low molecular weight species were indeed HA (supplemental Fig. 5). After electrophoresis, gels were stained with Stains-All®, and images were obtained using a ChemiDoc XRS imaging system (Bio-Rad). Changes in HA molecular mass distribution were assessed by densitometry using the Quantity One software (Bio-Rad) and results expressed as pixel intensity per relative front in each band.

Immunoblotting

Aliquots containing equal amounts of protein were diluted in Laemmli sample buffer, electrophoresed on 4–15% acrylamide gels, and transferred to PVDF membranes. After blocking, membranes were incubated with anti-E-cadherin antibodies (1 μg/ml, Santa Cruz Biotechnology) followed by the corresponding alkaline phosphatase-conjugated secondary antibody (Kirkegaard & Perry Laboratories); β-actin (0.5 μg/ml, Santa

Cruz Biotechnology) was used as a loading control. Membranes were developed using Lumi-Phos chemiluminescence (Thermo Fisher Scientific Inc., Waltham, MA), and images were obtained using a ChemiDoc XRS imaging system (Bio-Rad). Relative quantification of proteins was performed by determining the total pixel intensity associated with an individual band using Quantity One software (Bio-Rad).

RhoA Activation Assay

Cells were treated as above, and RhoA activation was measured using a G-LISA™ assay kit (Cytoskeleton, Inc.) following the manufacturer's instructions. This assay uses a 96-well plate coated with a protein that binds RhoA-GTP (active form) but not the inactive GDP-bound form. Results were expressed as changes to PBS control.

HA Affinity Chromatography

To confirm that the layilin used in our experiments binds to hyaluronan as reported previously (39), 0.8 μg of layilin (Novus, Littleton, CO) was added to HA-Sepharose prepared as described (51, 52) and incubated for 1 h at RT. After extensive washing with 0.5 M NaCl in PBS, beads were eluted with 1 mg/ml HA (35 kDa, R&D Systems). The specificity of the binding was confirmed by preincubating layilin with 6.5 kDa of HA or chondroitin sulfate (CS; both 1 mg/ml, 1 h room temperature) before loading to HA-Sepharose. The set of starting, flow-through, washing, and eluting samples were digested with 10 turbidity-reducing units/ml *Streptomyces* hyaluronidase (Seikagaku) at 60 °C for 2 h, electrophoresing in 10% PAGE, and transferring for WB analysis using mouse anti-layilin antibodies (Novus). A second set was run without hyaluronidase digestion and in nondenaturing conditions (no SDS, DTT, or heat) to visualize changes in mobility of the layilin-HA complexes.

Layilin Knockdown

Layilin expression was specifically knocked down using lentivirus expressing small interfering RNA (siRNA) generated as described (37, 53). Briefly, pLKO.1 plasmids encoding nontargeting (NT) or anti-layilin short hairpin RNAs were purchased from Open Biosystems, Inc. (Huntsville, AL). Replication-deficient lentiviruses were prepared by co-transfecting vector and packaging DNAs, pMDLg/pRRE#54 pRSV-Rev and pMDLgVSVG, into HEK 293T cells by calcium phosphate co-precipitation. Viruses were collected daily for 3 days, concentrated using 11% polyethylene glycol, and titers estimated by measuring p24 by ELISA (PerkinElmer Life Sciences). Undifferentiated NHBE cells were exposed to virus in bronchial epithelial growth medium for 24 h. Infected cells were selected with puromycin (1 μg/ml in bronchial epithelial growth medium) for 48 h and cultured in ALI conditions as described above. Cells were fully re-differentiated before experiments.

Statistical Analysis

Data are expressed as means ± S.E. The Shapiro-Wilk test was used for normality analysis. Differences between multiple groups were tested for significance using a one-way analysis of variance followed by Tukey test or Kruskal-Wallis analysis of variance on ranks. Significance was accepted at $p < 0.05$.

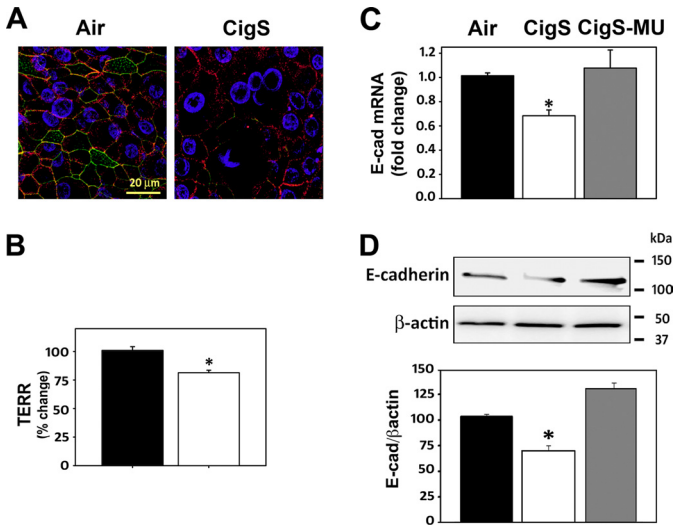

FIGURE 1. **CigS induces epithelial barrier disruption that is mediated by HA.** NHBE cultures were exposed to air or *CigS,* and epithelial integrity was evaluated 24 h later by immunofluorescence and TEER. *A,* representative picture ($n = 3$) visualizing E-cadherin (*red*) and F-actin (*green*). Nuclei were labeled with DAPI (*blue*). *B,* changes in TEER. *Asterisk* indicates $p < 0.001$ in CigS-exposed cells (*open bar*) with respect to air (*filled bar, n* = 5). The role of HA in CigS-induced E-cadherin gene and protein expression was tested by treating cells with MU 48 h before being exposed to air or CigS. *C,* E-cadherin mRNA measured by qPCR in cells exposed to CigS (*open bar*), CigS pretreated with MU (*gray bar*) or air (*filled bar*). *Graph* shows results expressed as mean ± S.E. fold change with respect to control (*filled bar*). *Asterisk* indicates $p < 0.05$ ($n = 6$). *D,* E-cadherin protein expression was evaluated by WB. *Top panel,* representative blot. *Bottom panel,* bands were quantified by densitometry ($n = 4$) and results expressed as mean ± S.E. of percentage of change with respect to air-exposed cells. *Asterisk* indicates $p < 0.001$.

RESULTS

In all results, "*n*" refers to the number of individual lung donors used to obtain cells for the primary cultures.

Exposure to Cigarette Smoke Results in Epithelial Barrier Disruption and Inhibition of E-cadherin Expression That Is Mediated by HA—Because chronic exposure to CigS is associated with increased epithelial permeability and decreased expression of proteins of the AJC *in vivo* and in cell lines (54), we assessed whether exposure to CigS resulted in changes in TEER and in the expression and/or distribution of AJC proteins. As depicted in Fig. 1*A*, CigS exposure resulted in apparent changes in cytoskeletal architecture (F-acting, *green*) and a loss of E-cadherin (*red*) immunolabeling at the cell membrane. Morphometric analysis ($n = 3$) evidenced a significant (~35%) reduction in the mean linear intercept (Lm/100 μm) count (7.1 ± 0.3 in smoked *versus* 10.8 ± 0.3 in air-exposed cells, $p < 0.001$). Decreased E-cadherin expression in CigS-exposed cells was accompanied by a significant reduction in TEER (Fig. 1*B*) from 100.3 ± 1.5 to 82.3 ± 1.5% compared with air control, $p < 0.001$ ($n = 5$), confirming that the increased epithelial permeability observed in smokers can be accurately reproduced in primary cultures grown at the ALI. Because HA reduces cell-cell adhesion in other cells (30, 34), we tested whether the HA present at the airway surface was involved in CigS-induced epithelial barrier disruption. For this purpose, HA synthesis was inhibited with MU (Fig. 1*C*) before exposure to CigS (*open bars*) or air (*filled bars*) as described under "Experimental Procedures." As shown in Fig. 1*C*, CigS exposure resulted in a significant reduction of E-cadherin gene expression ($n = 4$, 0.6 ± 0.1- *versus*

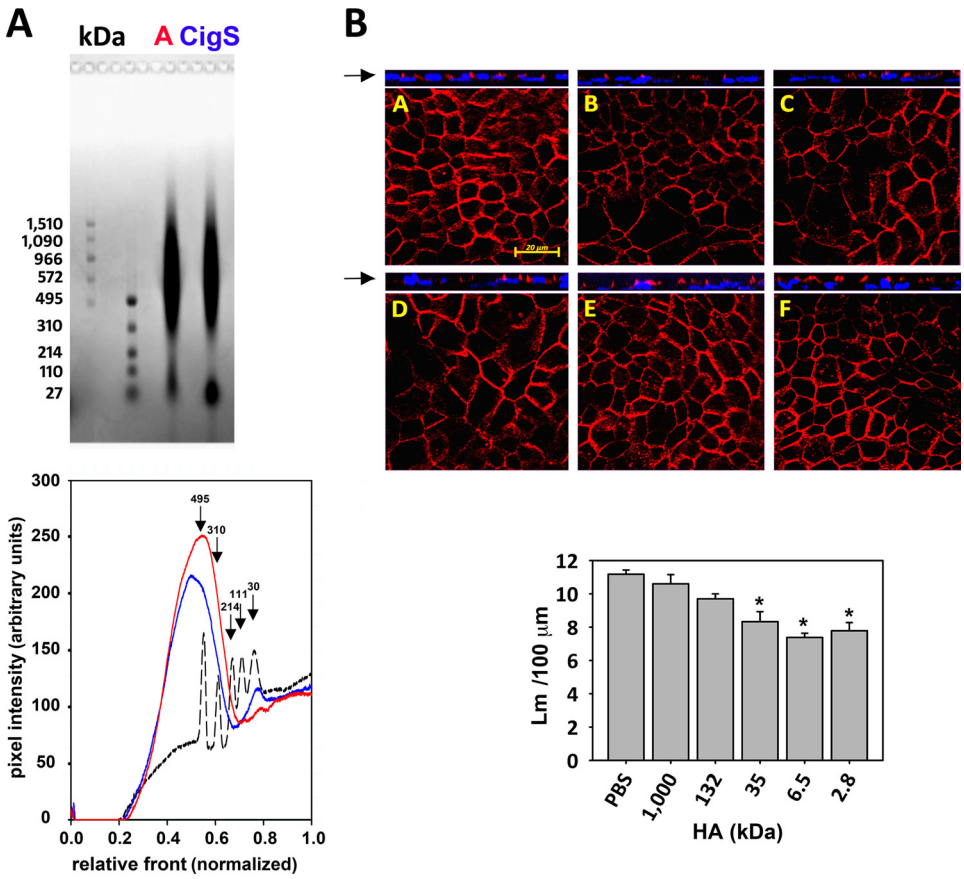

FIGURE 2. **Small HA fragments (oHA) are increased in apical secretions of NHBE cells and induce AJC disruption in a size-dependent manner.** *A,* apical secretions from NHBE cells were collected 24 h after exposure to CigS or air (*A*), digested with proteinase K and chondroitinase ABC, and HA molecular mass distribution was assessed by agarose electrophoresis as described under "Experimental Procedures." *Top panel,* image of a representative ($n = 4$) 0.7% agarose gel stained with StainsAll®. *Bottom panel,* densitometry analysis of image above. *Curves* depict samples exposed to air (*red*), CigS (*blue*), and molecular weight standards. The *arrows* point toward the peaks (*black dotted line*) generated by molecular weight standards used to calibrate the curve. *B,* immunofluorescence images of E-cadherin (*red*) distribution in NHBE cultures exposed to (*panel A*) PBS or HA of 2.8, 6.5, 35, 132, and 1000 kDa (*panels B–F*) for 24 h. *xy* plane (*lower panels*) for each image were taken at the level indicated by the *arrow* in the *z*-stack images (*upper panels*). Nuclei were visualized with DAPI. *Bottom panel,* quantification of AJC disruption by mean linear intercept (Lm, $n = 3$).

1.0 ± 0.1-fold changes; $p < 0.001$), although pretreatment with MU (*gray bars*) prevented these effects (1.1 ± 0.1). Protein expression was accordingly decreased by CigS exposure but not in cells pretreated with MU (70 ± 5 *versus* 118 ± 4% $n = 4$, $p < 0.001$). A representative blot and densitometry analysis ($n = 4$) are shown in Fig. 1*D*. These data strongly suggest that HA is involved in the increased epithelial permeability triggered by CigS.

Exposure to HA Results in Loss of E-cadherin in Apical Junctions That Is Size-dependent—After confirming that CigS exposure resulted in apical HA depolymerization, we tested if epithelial disruption by CigS could be mimicked by exposing them to HA and if the size of HA affected the response. Molecular mass distribution was assessed in apical washes of cells exposed to air or CigS (Fig. 2*A*). The appearance of the HA fragment (<35 kDa) is visualized in Fig. 2*A* and accompanied by a decrease in higher molecular species in CigS-exposed cells as evident in the gel image (*top panel*) and in the graph depicting densitometry analysis (*bottom panel*). Next, as shown in Fig. 2*B*, NHBE cells were apically exposed to PBS (control) or to 50 μg/ml of HA of different sizes (from 1.9 to 1,000 kDa) as described under "Experimental Procedures." We found that exposure to HA fragments of 2.8, 6.5, and 35 kDa reduced the staining (*top panel*) for E-cadherin (Fig. 2*B, panels B–D*) and resulted in a lower number of intercepts between ~25 and 35% with respect to PBS (Fig. 2*B, panel A*) with Lm/100-μm counts of 8.3 ± 0.5, 7.8 ± 0.3, and 8.7 ± 0.5, respectively (all $p \leq 0.002$), *versus* 11.2 ± 0.3, $n = 3$ (*bottom panel*). When HA of higher molecular weight was used (132 and 1000 kDa), we found minimal or no effect on E-cadherin distribution (Fig. 2*B*, *panels E* and *F*), and the number of intercepts were similar to PBS control (Fig. 2*B, panel A*) where Lm values were 9.7 ± 0.3 and 10.6 ± 0.6, respectively (Fig. 2*B*, *bottom panel*). Additional experiments using HA of 1.9 (HA10), 70, or 866 kDa (supplemental Fig. 6) further confirmed that cell exposure to HA of ≤70 kDa resulted in epithelial barrier disruption, suggesting that a direct or indirect interaction with a specific receptor was involved in the observed response.

oHA Down-regulates E-cadherin Expression, Increases Transepithelial Resistance and Paracellular Permeability—Based on the size-dependent response detailed above, we chose HA of 6.5 kDa (oHA) to assess changes in airway epithelial barrier function. NHBE cultures were exposed to PBS or oHA, and E-cadherin gene and protein expression were assessed by qPCR, WB, and immunofluorescence. Results depicted in Fig. 3*A* show that oHA significantly down-regulated E-cadherin mRNA expression when compared with PBS ($n = 3$, 0.6 ± 0.1- *versus* 1.0 ±

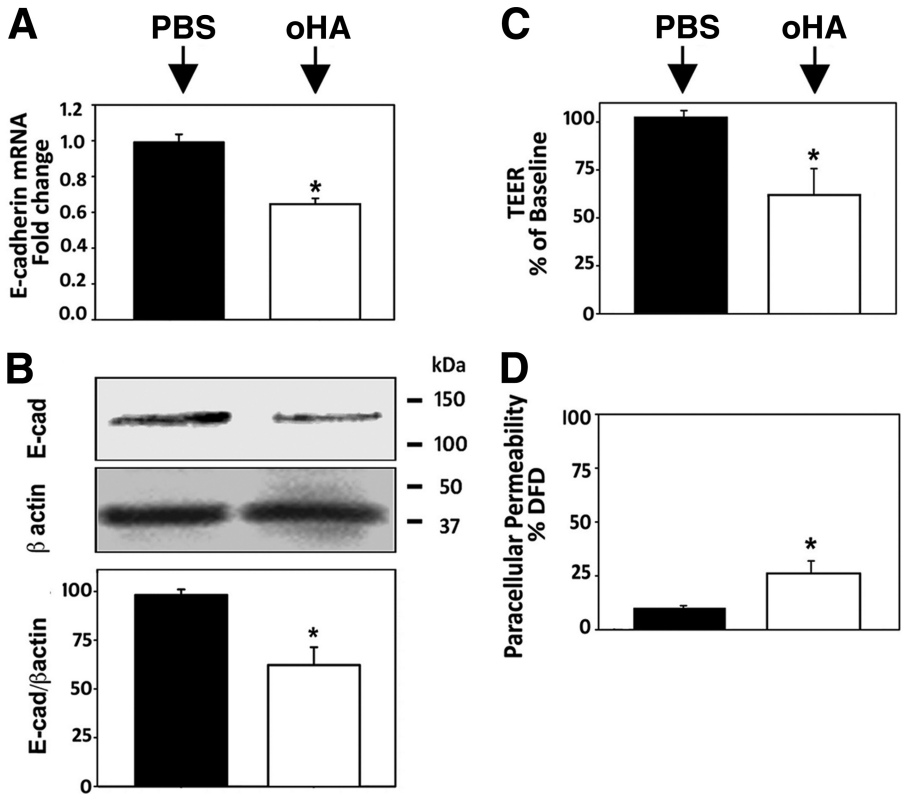

FIGURE 3. **oHA exposure results in decreased E-cadherin gene and protein expression and increased airway epithelial permeability.** *A,* E-cadherin mRNA was measured by qPCR in cells apically exposed to oHA (*open bars*) or PBS (*filled bars*). Results expressed as fold change show means ± S.E. with respect to PBS. *Asterisk* indicates $p < 0.05$ ($n = 3$). *B,* E-cadherin (*E-cad*) protein expression was evaluated by WB. *Top,* representative blot. *Bottom,* bands were quantified by densitometry ($n = 3$) and results expressed as means ± S.E. of percentage of change with respect to air-exposed cells. *Asterisk* indicates $p < 0.05$. *C, graph* shows TEER measurements in NHBE apically exposed to PBS or oHA. Measurements were recorded immediately before (*T*0) and 24 h after the initial treatment, and the percentage of change from *T*0 was expressed as means ± S.E. ($n = 5$). *D,* paracellular permeability to fluorescent dextran (~10 kDa) added to basolateral media and quantified in the apical washes. Results were expressed as percentage of dextran fluorescence diffusion (%DFD) compared with diffusion across empty filters (no cells), and *graph* shows means ± S.E. ($n = 5$) *Asterisk* indicates $p < 0.05$.

0.1-fold change, $p < 0.05$), and these results were accompanied by decreased protein expression. A representative WB and densitometry analysis of these experiments are shown in Fig. 3*B* (% change in oHA was 63 ± 9.3 *versus* 100 ± 3.0 in PBS, $n = 3$, $p < 0.05$). To assess if these changes were associated with changes in epithelial cell permeability, TEER was measured, and the results (Fig. 3*C*) show that oHA exposure significantly reduced TEER when compared with PBS (60.2 ± 7.0 *versus* 102.1 ± 2.4%; $n = 5$, $p < 0.05$). These changes correlated to an increased basal to apical paracellular flux of fluorescent dextran (Fig. 3*D*), where fluorescence diffusion (% DFD) was significantly increased in oHA-treated cells when compared with cells exposed to PBS ($n = 5$, 26.2 ± 5.7 *versus* 9.6 ± 1.2% DFD, $p < 0.05$), confirming that oHA is able to mimic CigS-induced effects in epithelial barrier function.

oHA Signals through RhoA/ROCK—Because small GTPases from Rho family are involved in the regulation of proteins of the AJC, we first tested if RhoA and ROCK were expressed in airway epithelium. Fig. 4*A* depicts images of NHBE cells labeled with antibodies against RhoA (*green*) and ROCK (*red*) that provide evidence that RhoA and ROCK are expressed in NHBE cells and localize at the apical and lateral domains (*yellow arrows*). To test if oHA is able to induce RhoA activation, NHBE cells were exposed to PBS (control) or oHA, and RhoA activation was assessed as described under "Experimental Procedures." Results depicted in Fig. 4*B* show that oHA induced significant RhoA activation compared with PBS ($n = 6$, 1.9 ± 0.2- *versus* 1.0 ± 0.1-fold, $p < 0.005$). To test if RhoA/ROCK pathway was involved in the decreased E-cadherin expression induced by oHA, cells were apically exposed to PBS or oHA in the presence or absence of the RhoA inhibitor C3 exoenzyme (C3) or the ROCK inhibitor Y27632. Images depicted in Fig. 4*C* show a reduction in E-cadherin staining at the cell membrane in oHA-treated cells that was prevented by C3 and Y27632 pretreatment (*top panel*). Morphometric analysis (*bottom panel*) revealed that oHA induced a reduction of ~30% in the number of E-cadherin strand intercepts when compared with PBS (7.8 ± 0.6 *versus* 11.2 ± 0.3; $n = 4$ $p < 0.001$) although pretreatment with C3 or Y27632 resulted in values comparable with PBS (11.0 ± 0.4 and 10.9 ± 0.4, respectively). These data point toward RhoA/ROCK as signaling effectors involved in E-cadherin inhibition triggered by oHA.

Layilin Is Expressed at the Apical Surface of Ciliated Epithelial Cells and Binds HA but Not Chondroitin Sulfate—Because layilin is a cell surface HA receptor (39) that interacts with proteins known to regulate cytoskeleton-plasma membrane interactions in polarized cell, and thus an ideal candidate to mediate increases in AJC disruption by HA, we used immunofluorescence and WB to test if layilin was expressed in respiratory epithelium. As depicted in Fig. 5, layilin (*red*) is expressed in the

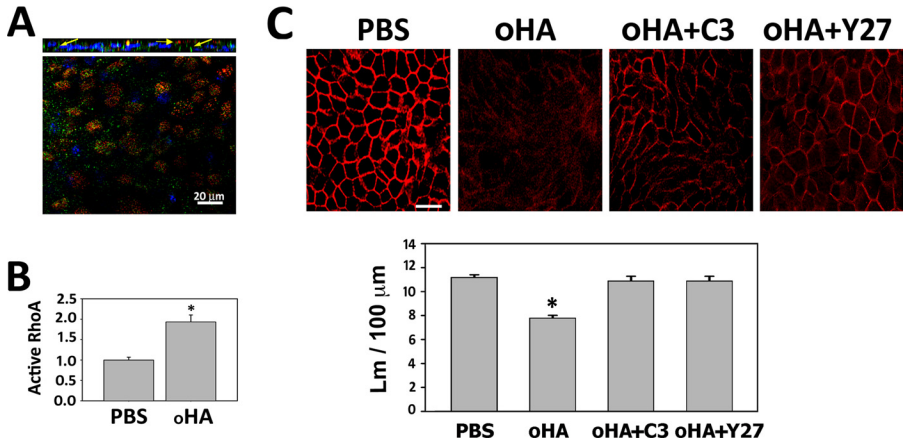

FIGURE 4. **RhoA/ROCK are expressed in NHBE cells and mediate AJC disruption triggered by oHA.** *A,* NHBE cells were fixed and double labeled using specific antibodies for RhoA (*green*) and ROCK (*red*). A representative immunofluorescence shows the apical and basolateral localization (*yellow arrows*). Nuclei were stained with DAPI (*blue*). *B,* RhoA activation determined by G-lisa 24 h after NHBE cells were exposed to PBS or oHA. Results are expressed as fold change respect to PBS, and *graph* shows means ± S.E. *Asterisk* indicates $p < 0.05$ ($n = 6$). *C, top panel,* E-cadherin distribution (*red*) assessed by immunofluorescence in NHBE cells exposed to PBS or oHA in the presence or the absence of a RhoA inhibitor (*C3*) or a ROCK kinase inhibitor (Y27632 (*Y27*)), *Bar,* 20 μm. *Bottom,* quantification of AJC disruption by mean linear intercept (Lm, $n = 4$). *Asterisk* indicates $p < 0.001$ respect to PBS.

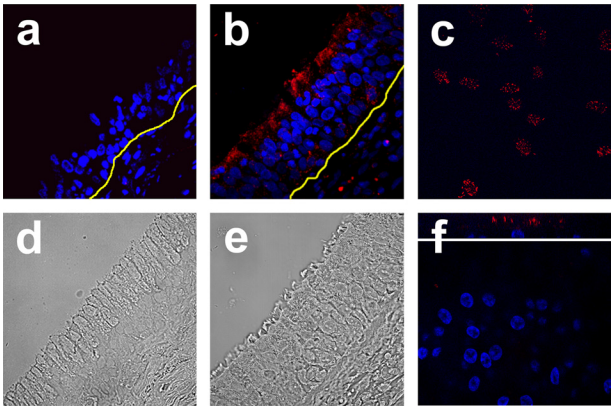

FIGURE 5. **HA receptor layilin is expressed apically in human airway epithelium.** Human tracheal tissue sections (*a, b, d,* and *e*) obtained from lung donors (representative image from $n = 4$) and NHBE cell cultures ($n = 4$; *c* and *f*) were labeled with specific mouse anti-human layilin (*b, c,* and *f*) or mouse IgG (nonimmune control, *a*), followed by secondary antibodies tagged with Alexa 555. A *yellow line* highlights the lamina propria separating epithelium from subepithelial matrix, and the corresponding differential interference contrast images are shown in *d* and *e*. NHBE cells were labeled as above, and image from *xy* planes were obtained at the apical (*c*) or the basolateral levels (*f*) that are accompanied with *z*-stack reconstruction at the top. *Bar,* 20 μm.

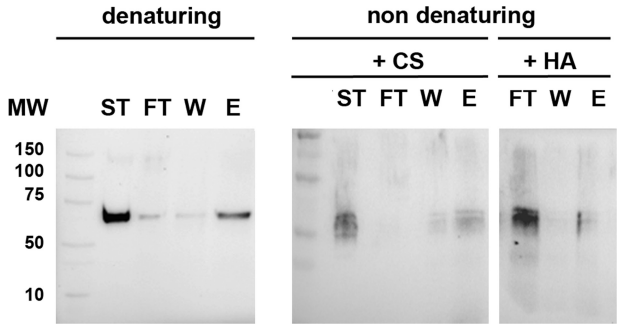

FIGURE 6. **Layilin specifically binds to HA and not chondroitin sulfate.** Layilin was loaded into HA-Sepharose as detailed under "Experimental Procedures," washed with 0.5 M NaCl in PBS, and eluted with HA 35 kDa in PBS. Experiment was repeated using layilin preincubated with CS or HA (6.5 kDa), and samples were analyzed by WB. Figure shows WB using antibodies against layilin. Samples were run in denaturating and nondenaturing conditions. Lines are molecular markers (*MW*), starting material (*ST*), flow-through (*FT*), high salt wash (*W*), and HA elution (*E*).

airway epithelium of human trachea. Fig. 5*a* depicts a nonimmune control of tracheal tissue, and the image in Fig. 5*b* shows that layilin is expressed at the airway epithelium, but more importantly, its localization is limited to the apical compartment. Fig. 5, *d* and *e*, shows differential interference contrast images corresponding to Fig. 5, *a* and *b*, respectively. Apical localization is also evident in NHBE cells (Fig. 5*c*) but not at the basolateral compartment (Fig. 5*f*). *z* axis reconstruction of the image depicted in Fig. 5*f* (*top panel*) confirms layilin expression at the apical surface of ciliated cells. We conclude that layilin is present and at the right location to interact with HA fragments released by CigS at the airway lumen. A representative blot of samples of NHBE cell lysates labeled with an antibody against human layilin as described in "Experimental Procedures" (supplemental Fig. 7) reveals two specific bands of ~52 and ~ 40 kDa that coincide with the reported size of layilin (40). We reproduced the affinity chromatography experiments reported by Bono *et al.* (39), evidencing that layilin is an HA-binding protein. We confirmed that layilin binds to immobilized HA and can be eluted with excess oHA. In contrast, when layilin was preincubated with HA, binding did not occur. An additional control shows that CS do not interfere with HA binding (as reported previously (39)). Visualization by WB (Fig. 6) summarizes the results of these experiments. Samples where run in denaturing and nondenaturing conditions, and the *lanes* in Fig. 6 are as follows: starting material (*ST*), flow-through (*FT*), high salt wash (*W*), and elution with HA (*E*). The changes in layilin mobility in nondenaturing conditions further confirmed that layilin is in fact an HA-binding protein that selectively binds HA but not CS.

Epithelial Disruption by CigS and oHA Is Mediated by the HA Receptor Layilin—To explore the participation of layilin in CigS and oHA-associated epithelial barrier disruption, its expression was knocked down using lentivirus-expressing small interference RNA (siLy). Using these constructs, we obtained ~60% of layilin knockdown when compared with infected cells carrying a nontargeting sequence (NTsi, 0.4 ± 0.1- *versus* 1.0 ± 0.1-fold, $p < 0.005$) but did not decrease the expression of other relevant

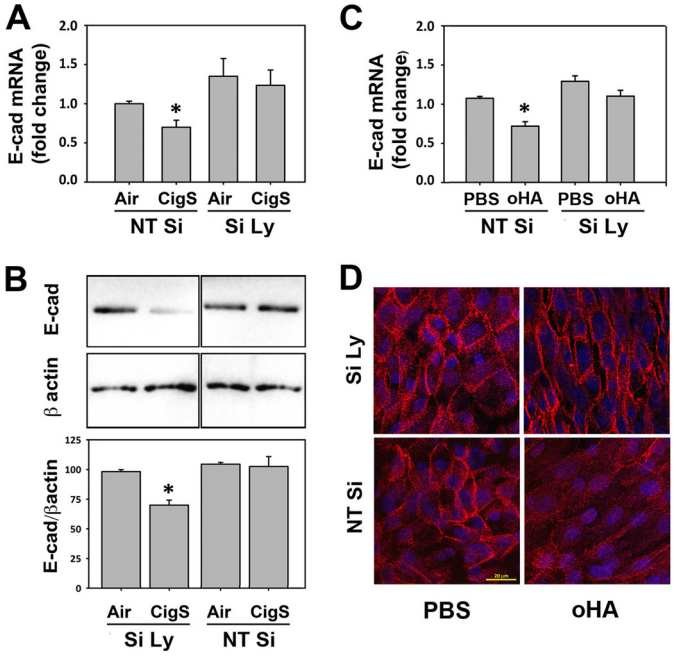

FIGURE 7. **Layilin knockdown protects NHBE cells from CigS and oHA-induced E-cadherin down-regulation.** Cultures were infected with lentivirus expressing siRNA for layilin (*siLy*) or nontargeting siRNA (*NTsi*) and after full differentiation were exposed to CigS or air. *A,* E-cadherin mRNA expression was evaluated by qPCR, and results were expressed as fold change with respect to air. *B,* representative blot (*top*) of E-cadherin protein expression and results are normalized to β-actin (*bottom*), means ± S.E. *Asterisk* indicates $p < 0.001$ with respect to air-exposed cultures ($n = 3$). *C,* NHBE cells infected with siLy or NTsi were exposed to PBS or oHA (6.5 kDa). E-cadherin mRNA expression was evaluated by qPCR, and results are expressed as fold changes from NTsi PBS. *Asterisk* indicates $p < 0.001$ ($n = 4$). *D* representative immunofluorescence image depicting E-cadherin distribution in cells infected with siLy or NTsi controls exposed to oHA.

targets such as HAS2, HAS3, CD44, or RHAMM (supplemental Fig. 8). We did observe a significant increase in RHAMM expression in siLy-infected cells when compared with NTsi (2.5 ± 0.6- *versus* 1.0 ± 0.1-fold, $p < 0.005$), suggesting that layilin and RHAMM are part of a redundant system, likely associated with HA signaling-independent of Rho/ROCK. Cultures infected with siLy or NTsi were exposed to air or CigS, and E-cadherin expression was determined by qPCR. Fig. 7*A* summarizes the results of these experiments. As observed in the cells infected with non-targeting siRNA (NTsi) exposed to CigS, expressed significantly less E-cadherin mRNA when compared with NTsi cells exposed to air (0.7 ± 0.1- *versus* 1.1 ± 0.1-fold change; $n = 6$, $p = 0.001$). In contrast, cells infected with siLy were protected, and CigS exposure did not affect E-cadherin gene expression. Results in siLy cells were comparable with the expression observed in cells exposed to air (1.4 ± 0.3 *versus* 1.2 ± 0.3 $n = 6$). A representative blot (Fig. 7*B*) shows that changes in mRNA were accompanied by similar results in protein expression. In NTsi cells exposed to CigS, we observed decreased protein levels, but in siLy-infected cells E-cadherin amounts remained virtually unchanged (71.7 ± 4.2 in nontargeting *versus* 101.3 ± 1.5 in siLy), both compared with NTsi air-exposed cells (100 ± 1.6; $p < 0.05$). To confirm that these effects were indeed mediated by HA, siLy- or NTsi-infected cells were exposed to oHA or PBS, and the E- cadherin gene and protein expression were assessed as detailed under "Experimental Procedures." Results depicted in Fig. 7*C* show that E-cadherin mRNA expression was reduced in NTsi cells exposed to oHA when compared with PBS (0.7 ± 0.1- *versus* 1.0 ± 0.1-fold change; $n = 4$ $p < 0.05$), but this inhibition did not occur in cells infected with siLy (1.3 ± 0.2- *versus* 1.2 ± 0.2-fold change; $n = 4$). Accordingly, the loss of E-cadherin immunostaining in NTsi cells exposed to oHA was partially prevented in cells expressing siLy (Fig. 7*D*). These data provide strong evidence that layilin functions as an HA cell surface receptor in airway epithelial cells and its responsible for the increased epithelial permeability induced by CigS and oHA.

DISCUSSION

The airway epithelium is the first line of defense providing a physical barrier to the environment. Besides its barrier/fence function, it plays a key role in regulating the underlying tissue response to external stimuli (55). The harmful effects of cigarette smoke start with epithelial damage followed by an inflammatory response that propagates into the subepithelial tissue (56). Exposure to CigS leads to increased paracellular permeability (6–10) that potentiates and sustains airway inflammation (57) in respiratory diseases such as COPD and asthma (3, 4, 10). In fact, airway epithelial permeability and the number of inflammatory cells in the bronchial lumen are increased in smokers and passive smokers (58–62).

Although increased epithelial permeability is a known harmful effect of CigS, the molecular mechanisms orchestrating the loss of epithelia cell-cell contact have not been fully characterized. The integrity of the epithelial barrier is maintained by the AJC that separates apical from basolateral domains, providing mechanical strength to the epithelial layer (63, 64) and selectively regulating the movement of water, molecules, and inflammatory cells through the paracellular space.

Here, we report that exposure to CigS generated by one cigarette is enough to down-regulate E-cadherin gene expression and to alter AJC architecture in primary cultures of NHBE cells. Consistent with these findings, Shaykhiev *et al.* (54) recently showed that a profound down-regulation of the entire molecular AJC machinery, particularly claudin and E-cadherin, is observed in healthy smokers when compared with nonsmokers. Our results are also in agreement with a previous report indicating that CigS extract in BEAS-2B and 16HBE14o cell lines facilitates allergen penetration by increasing epithelial permeability (54, 65).

HA is a glycosaminoglycan that is normally found as a high molecular weight polymer attached to the apical membrane of bronchial epithelium (20, 21), soluble in tracheobronchial secretions (20, 66, 67) and in the subepithelial matrix (68). HA is involved in a broad range of processes that involve structural changes in AJC. For instance, HA mediates the epidermal response to barrier injury by accelerating terminal differentiation (69), cell differentiation, and epithelial-mesenchymal transition (70–74). Cywes and Wessels (75) have shown that tissue invasion by group A *Streptococcus* is due to intercellular junction disruption mediated by capsule-associated HA. We and others have reported that there is an increased HA degradation with appearance of soluble HA fragments in smokers and in cells exposed to oxidative stress (36, 37, 76). Here, we show that this effect can be mimicked by directly exposing primary cul-

tures to CigS. We also show that apical exposure to HA of <70 kDa, but not a higher molecular mass, induced architectural changes of the AJC that are accompanied by altered distribution and down-regulation of the E-cadherin gene and protein expression. These changes were associated with decreased trans-epithelial resistance and increased paracellular permeability and agreed with studies in other tissues where exposure to oHA induced vascular barrier disruption, although high molecular weight prevented pulmonary vascular leakiness (30). The size-dependent effects are broadly documented, with high molecular weight exerting anti-inflammatory and immunosuppressive effects, whereas fragments stimulate gene expression and protein synthesis of pro-inflammatory mediators (77, 78).

The mechanisms responsible for regulation of epithelial permeability are quite complex, involving a number of biochemical and cellular pathways/events (14). In BEAS-2B and 16HBE14o cell lines ZO-1 disassembly after exposure to CigS extract was mediated by the EGF receptor-44/42MAPK pathway (65), but in monolayers of Calu-3 cells, mainstream CigS induced a rapid and transient permeability increase with ZO-1-occludin dissociation mediated by tyrosine kinase phosphorylation followed by ROCK activation (79, 80). Here, we show that RhoA/ROCK, expressed in fully differentiated NHBE cells, are activated by CigS and oHA and that both RhoA and ROCK inhibitors protected NHBE cells from AJC architectural changes induced by oHA. Inhibition of HA synthesis by 4-methylumbelliferone provided key evidence that depolymerization of endogenous HA was responsible for the epithelial barrier disruption triggered by CigS. Although an estimation of the exact concentration and size distribution of HA in the microenvironment close to the cell membrane is virtually impossible with the current technology, the amount of exogenous HA used in our experiments is about 5–10 times higher than the concentration measured in the airway secretions of smokers. This concentration is enough to compete out high molecular weight species present at the airway surface and to gain access to cell surface receptors, which we believe is consistent with physiological conditions. We have shown, using fluorophore-assisted carbohydrate electrophoresis, that airway secretions contain low concentrations of CS, although heparan sulfate is not detected (20). Immunolabeling confirmed that heparan sulfate is limited to subepithelial tissue (20), and thus it is unlikely that these glycosaminoglycans contribute or confound the results reported here.

We determined that loss of cell-cell contact was mediated by layilin, a membrane HA receptor with an extracellular domain that is homologous to the carbohydrate-recognition domains of C-type lectin, that we found to be expressed apically in airway epithelial cells. We confirmed that layilin specifically binds HA (39) as reported previously. What pointed toward layilin as an ideal HA receptor to be involved epithelial permeability is that it is known to interact with members of the ezrin, radixin, and moesin proteins (81) that are key regulators of cytoskeleton-plasma membrane interactions in polarized cell. CD44 and RHAMM are two of the better characterized HA receptors in airway epithelial cells (19, 21, 82–84), but in intact epithelium CD44 expression is restricted to the basolateral domain (83, 85, 86) and thus, at least initially, cannot be accessed by fragments released during luminal HA degradation. RHAMM is apically expressed (19, 21) but lacks a cytoplasmic domain. We have shown that RHAMM interacts with RON to regulate ciliary beat frequency (19). Because RHAMM/RON-induced pathways include phosphatidylinositol 3-kinase (PI3K), mitogen-activated protein kinase (MAPK), and c-Jun N-terminal kinase (87) but not Rho/ROCK, it is unlikely to be involved in the signaling pathway that results in E-cadherin inhibition. Knockdown studies using cells infected with lentivirus carrying siLy evidenced higher E-cadherin expression than cells infected with nontargeting sequences, and more importantly, knockdown cells did not respond with decreased E-cadherin expression when exposed to CigS or oHA. An unexpected finding was that RHAMM expression was significantly increased in siLy-infected cells, suggesting the existence of a redundant signaling pathway shared by layilin and RHAMM but unlikely to be associated with the signaling events that affected E-cadherin.

In smokers and in respiratory inflammatory diseases associated with abnormal epithelial barrier function, reactive oxygen species and Hyal2 operate in a coordinated manner to depolymerize HA at the airway lumen (20, 88). This work provides strong evidence that hyaluronan fragments generated by CigS bind to layilin and signal through RhoA/ROCK to inhibit E-cadherin gene and protein expression. The loss of cell-cell contact ultimately results in increased epithelial permeability subjecting the subepithelial tissue to exogenous insults. Thus, it is tempting to hypothesize that the HA that blankets the airway surface functions as a master switch, able to protect or disrupt the epithelial barrier in its high *versus* low molecular weight forms. Our results suggest that the HA receptor layilin plays an important role regulating epithelial permeability and that HA depolymerization by CigS is an initial and necessary event driving the inflammatory response to inhaled cigarette smoke.

Acknowledgments—We thank Drs. Gregory Conner and Matthias Salathe for continuous support. We also thank Gabriel Gaidosh and the Adrienne Arsht Retinal Degeneration Research Laboratory, the Analytical Imaging Core, the Life Alliance Organ Recovery Agency, and the Histology Laboratory from Sylvester Comprehensive Cancer Center, all at the University of Miami, Miller School of Medicine.

REFERENCES

1. Hogg, J. C., and Timens, W. (2009) The pathology of chronic obstructive pulmonary disease. *Annu. Rev. Pathol.* **4,** 435–459
2. Mason, R. J., Buist, A. S., Fisher, E. B., Merchant, J. A., Samet, J. M., and Welsh, C. H. (1985) Cigarette smoking and health. *Am. Rev. Respir. Dis.* **132,** 1133–1136
3. Jindal, S. K., and Gupta, D. (2004) The relationship between tobacco smoke and bronchial asthma. *Indian J. Med. Res.* **120,** 443–453
4. Kjellman, N. I. (1981) Effect of parental smoking on IgE levels in children. *Lancet* **1,** 993–994
5. Miyoshi, J., and Takai, Y. (2008) Structural and functional associations of apical junctions with cytoskeleton. *Biochim. Biophys. Acta* **1778,** 670–691
6. Kennedy, S. M., Elwood, R. K., Wiggs, B. J., Paré, P. D., and Hogg, J. C. (1984) Increased airway mucosal permeability of smokers. Relationship to airway reactivity. *Am. Rev. Respir. Dis.* **129,** 143–148
7. Rusznak, C., Mills, P. R., Devalia, J. L., Sapsford, R. J., Davies, R. J., and Lozewicz, S. (2000) Effect of cigarette smoke on the permeability and IL-1β and sICAM-1 release from cultured human bronchial epithelial cells of never-smokers, smokers, and patients with chronic obstructive pulmonary disease. *Am. J. Respir. Cell Mol. Biol.* **23,** 530–536

8. Beadsmoore, C., Cheow, H. K., Szczepura, K., Ruparelia, P., and Peters, A. M. (2007) Healthy passive cigarette smokers have increased pulmonary alveolar permeability. *Nucl. Med. Commun.* **28,** 75–77
9. Yates, D. H., Havill, K., Thompson, M. M., Rittano, A. B., Chu, J., and Glanville, A. R. (1996) Sidestream smoke inhalation decreases respiratory clearance of 99mTc-DTPA acutely. *Aust. N. Z. J. Med.* **26,** 513–518
10. Rusznak, C., Sapsford, R. J., Devalia, J. L., Justin John, R., Hewitt, E. L., Lamont, A. G., Wood, A. J., Shah, S. S., Davies, R. J., and Lozewicz, S. (1999) Cigarette smoke potentiates house dust mite allergen-induced increase in the permeability of human bronchial epithelial cells *in vitro*. *Am. J. Respir. Cell Mol. Biol.* **20,** 1238–1250
11. Pryor, W. A., and Stone, K. (1993) Oxidants in cigarette smoke. Radicals, hydrogen peroxide, peroxynitrate, and peroxynitrite. *Ann. N.Y. Acad. Sci.* **686,** 12–27
12. Rahman, I., and MacNee, W. (1996) Role of oxidants/antioxidants in smoking-induced lung diseases. *Free Radic. Biol. Med.* **21,** 669–681
13. Jeffery, P. K. (1992) Histological features of the airways in asthma and COPD. *Respiration* **59,** 13–16
14. Matter, K., and Balda, M. S. (2003) Signaling to and from tight junctions. *Nat. Rev. Mol. Cell Biol.* **4,** 225–236
15. Samarin, S. N., Ivanov, A. I., Flatau, G., Parkos, C. A., and Nusrat, A. (2007) Rho/Rho-associated kinase-II signaling mediates disassembly of epithelial apical junctions. *Mol. Biol. Cell* **18,** 3429–3439
16. Hopkins, A. M., Walsh, S. V., Verkade, P., Boquet, P., and Nusrat, A. (2003) Constitutive activation of Rho proteins by CNF-1 influences tight junction structure and epithelial barrier function. *J. Cell Sci.* **116,** 725–742
17. Fraser, J. R., Laurent, T. C., and Laurent, U. B. (1997) Hyaluronan. Its nature, distribution, functions, and turnover. *J. Intern. Med.* **242,** 27–33
18. Casalino-Matsuda, S. M., Monzón, M. E., and Forteza, R. M. (2006) Epidermal growth factor receptor activation by epidermal growth factor mediates oxidant-induced goblet cell metaplasia in human airway epithelium. *Am. J. Respir. Cell Mol. Biol.* **34,** 581–591
19. Manzanares, D., Monzon, M. E., Savani, R. C., and Salathe, M. (2007) Apical oxidative hyaluronan degradation stimulates airway ciliary beating via RHAMM and RON. *Am. J. Respir. Cell Mol. Biol.* **37,** 160–168
20. Monzon, M. E., Casalino-Matsuda, S. M., and Forteza, R. M. (2006) Identification of glycosaminoglycans in human airway secretions. *Am. J. Respir. Cell Mol. Biol.* **34,** 135–141
21. Forteza, R., Lieb, T., Aoki, T., Savani, R. C., Conner, G. E., and Salathe, M. (2001) Hyaluronan serves a novel role in airway mucosal host defense. *FASEB J.* **15,** 2179–2186
22. Casalino-Matsuda, S. M., Monzon, M. E., Day, A. J., and Forteza, R. M. (2009) Hyaluronan fragments/CD44 mediate oxidative stress-induced MUC5B up-regulation in airway epithelium. *Am. J. Respir. Cell Mol. Biol.* **40,** 277–285
23. Lauer, M. E., Fulop, C., Mukhopadhyay, D., Comhair, S., Erzurum, S. C., and Hascall, V. C. (2009) Airway smooth muscle cells synthesize hyaluronan cable structures independent of inter-α-inhibitor heavy chain attachment. *J. Biol. Chem.* **284,** 5313–5323
24. Cantor, J. O., and Nadkarni, P. P. (2006) Hyaluronan. The Jekyll and Hyde molecule. *Inflamm. Allergy Drug Targets* **5,** 257–260
25. Garantziotis, S., Li, Z., Potts, E. N., Kimata, K., Zhuo, L., Morgan, D. L., Savani, R. C., Noble, P. W., Foster, W. M., Schwartz, D. A., and Hollingsworth, J. W. (2009) Hyaluronan mediates ozone-induced airway hyperresponsiveness in mice. *J. Biol. Chem.* **284,** 11309–11317
26. Day, A. J. (2001) Understanding Hyaluronan-Protein Interactions. *Glycoforum, Hyaluronan Today,*
27. Zhu, L., Zhuo, L., Kimata, K., Yamaguchi, E., Watanabe, H., Aronica, M. A., Hascall, V. C., and Baba, K. (2010) Deficiency in the serum-derived hyaluronan-associated protein-hyaluronan complex enhances airway hyper-responsiveness in a murine model of asthma. *Int. Arch. Allergy Immunol.* **153,** 223–233
28. Garantziotis, S., Zudaire, E., Trempus, C. S., Hollingsworth, J. W., Jiang, D., Lancaster, L. H., Richardson, E., Zhuo, L., Cuttitta, F., Brown, K. K., Noble, P. W., Kimata, K., and Schwartz, D. A. (2008) Serum inter-α-trypsin inhibitor and matrix hyaluronan promote angiogenesis in fibrotic lung injury. *Am. J. Respir. Crit. Care Med.* **178,** 939–947
29. de la Motte, C. A., Hascall, V. C., Drazba, J., Bandyopadhyay, S. K., and Strong, S. A. (2003) Mononuclear leukocytes bind to specific hyaluronan structures on colon mucosal smooth muscle cells treated with polyinosinic acid:polycytidylic acid. Inter-α-trypsin inhibitor is crucial to structure and function. *Am. J. Pathol.* **163,** 121–133
30. Singleton, P. A., Dudek, S. M., Ma, S. F., and Garcia, J. G. (2006) Transactivation of sphingosine 1-phosphate receptors is essential for vascular barrier regulation. Novel role for hyaluronan and CD44 receptor family. *J. Biol. Chem.* **281,** 34381–34393
31. Murai, T., Miyazaki, Y., Nishinakamura, H., Sugahara, K. N., Miyauchi, T., Sako, Y., Yanagida, T., and Miyasaka, M. (2004) Engagement of CD44 promotes Rac activation and CD44 cleavage during tumor cell migration. *J. Biol. Chem.* **279,** 4541–4550
32. Sugahara, K. N., Murai, T., Nishinakamura, H., Kawashima, H., Saya, H., and Miyasaka, M. (2003) Hyaluronan oligosaccharides induce CD44 cleavage and promote cell migration in CD44-expressing tumor cells. *J. Biol. Chem.* **278,** 32259–32265
33. Kuwabara, H., Yoneda, M., Hayasaki, H., Nakamura, T., and Shibayama, Y. (2011) A hyaluronan synthase suppressor, 4-methylumbelliferone, inhibits the tumor invasion associated with N-cadherin decreasement. *Pathol. Int.* **61,** 262–263
34. Bharadwaj, A. G., Goodrich, N. P., McAtee, C. O., Haferbier, K., Oakley, G. G., Wahl, J. K., 3rd, and Simpson, M. A. (2011) Hyaluronan suppresses prostate tumor cell proliferation through diminished expression of N-cadherin and aberrant growth factor receptor signaling. *Exp. Cell Res.* **317,** 1214–1225
35. Yamazaki, K., Fukuda, K., Matsukawa, M., Hara, F., Yoshida, K., Akagi, M., Munakata, H., and Hamanishi, C. (2003) Reactive oxygen species depolymerize hyaluronan. Involvement of the hydroxyl radical. *Pathophysiology* **9,** 215–220
36. McDevitt, C. A., Beck, G. J., Ciunga, M. J., and O'Brien, J. (1989) Cigarette smoke degrades hyaluronic acid. *Lung* **167,** 237–245
37. Monzon, M. E., Fregien, N., Schmid, N., Falcon, N. S., Campos, M., Casalino-Matsuda, S. M., and Forteza, R. M. (2010) Reactive oxygen species and hyaluronidase 2 regulate airway epithelial hyaluronan fragmentation. *J. Biol. Chem.* **285,** 26126–26134
38. Bracke, K. R., Dentener, M. A., Papakonstantinou, E., Vernooy, J. H., Demoor, T., Pauwels, N. S., Cleutjens, J., van Suylen, R., Joos, G. F., Brusselle, G. G., and Wouters, E. F. (2010) Enhanced deposition of low-molecular-weight hyaluronan in lungs of cigarette smoke-exposed mice. *Am. J. Respir. Cell Mol. Biol.* **42,** 753–761
39. Bono, P., Rubin, K., Higgins, J. M., and Hynes, R. O. (2001) Layilin, a novel integral membrane protein, is a hyaluronan receptor. *Mol. Biol. Cell* **12,** 891–900
40. Borowsky, M. L., and Hynes, R. O. (1998) Layilin, a novel talin-binding transmembrane protein homologous with C-type lectins, is localized in membrane ruffles. *J. Cell Biol.* **143,** 429–442
41. Chen, Z., Zhuo, W., Wang, Y., Ao, X., and An, J. (2008) Down-regulation of layilin, a novel hyaluronan receptor, via RNA interference, inhibits invasion and lymphatic metastasis of human lung A549 cells. *Biotechnol. Appl. Biochem.* **50,** 89–96
42. Nlend, M. C., Bookman, R. J., Conner, G. E., and Salathe, M. (2002) Regulator of G-protein signaling protein 2 modulates purinergic calcium and ciliary beat frequency responses in airway epithelia. *Am. J. Respir. Cell Mol. Biol.* **27,** 436–445
43. Bernacki, S. H., Nelson, A. L., Abdullah, L., Sheehan, J. K., Harris, A., Davis, C. W., and Randell, S. H. (1999) Mucin gene expression during differentiation of human airway epithelia *in vitro*. Muc4 and Muc5b are strongly induced. *Am. J. Respir. Cell Mol. Biol.* **20,** 595–604
44. Aufderheide, M., and Gressmann, H. (2008) Mutagenicity of native cigarette mainstream smoke and its gas/vapour phase by use of different tester strains and cigarettes in a modified Ames assay. *Mutat. Res.* **656,** 82–87
45. Cereijido, M., Shoshani, L., and Contreras, R. G. (2002) in *Cell-Cell Interactions* (Fleming, T. P., ed) 2nd Ed., pp. 71–91, Oxford University Press, New York
46. Thurlbeck, W. M. (1967) Measurement of pulmonary emphysema. *Am. Rev. Respir. Dis.* **95,** 752–764
47. Livak, K. J., and Schmittgen, T. D. (2001) Analysis of relative gene expression data using real time quantitative PCR and the $2(-\Delta\Delta C(T))$ method.

Methods **25,** 402–408
48. Casalino-Matsuda, S. M., Monzon, M. E., Conner, G. E., Salathe, M., and Forteza, R. M. (2004) Role of hyaluronan and reactive oxygen species in tissue kallikrein-mediated epidermal growth factor receptor activation in human airways. *J. Biol. Chem.* **279,** 21606–21616
49. Prabhakar, V., Capila, I., Bosques, C. J., Pojasek, K., and Sasisekharan, R. (2005) Chondroitinase ABC I from *Proteus vulgaris*. Cloning, recombinant expression, and active site identification. *Biochem. J.* **386,** 103–112
50. Lee, H. G., and Cowman, M. K. (1994) An agarose gel electrophoretic method for analysis of hyaluronan molecular weight distribution. *Anal. Biochem.* **219,** 278–287
51. Tengblad, A. (1979) Affinity chromatography on immobilized hyaluronate and its application to the isolation of hyaluronate binding properties from cartilage. *Biochim. Biophys. Acta* **578,** 281–289
52. Forteza, R., Lauredo, I., Abraham, W. M., and Conner, G. E. (1999) Bronchial tissue kallikrein activity is regulated by hyaluronic acid binding. *Am. J. Respir. Cell Mol. Biol.* **21,** 666–674
53. Schmid, A., Sutto, Z., Schmid, N., Novak, L., Ivonnet, P., Horvath, G., Conner, G., Fregien, N., and Salathe, M. (2010) Decreased soluble adenylyl cyclase activity in cystic fibrosis is related to defective apical bicarbonate exchange and affects ciliary beat frequency regulation. *J. Biol. Chem.* **285,** 29998–30007
54. Shaykhiev, R., Otaki, F., Bonsu, P., Dang, D. T., Teater, M., Strulovici-Barel, Y., Salit, J., Harvey, B. G., and Crystal, R. G. (2011) Cigarette smoking reprograms apical junctional complex molecular architecture in the human airway epithelium *in vivo*. *Cell. Mol. Life Sci.* **68,** 877–892
55. Knight, D. A., Stewart, G. A., and Thompson, P. J. (1994) The respiratory epithelium and airway smooth muscle homeostasis: its relevance to asthma. *Clin. Exp. Allergy* **24,** 698–706
56. Holgate, S. T. (2002) Airway inflammation and remodeling in asthma. Current concepts. *Mol. Biotechnol.* **22,** 179–189
57. Anderson, J. M., and Van Itallie, C. M. (1995) Tight junctions and the molecular basis for regulation of paracellular permeability. *Am. J. Physiol.* **269,** G467–G475
58. Walker, D. C., and Burns, A. R. (1988) The mechanism of cigarette smoke induced increased epithelial permeability in guinea pig airways. *Prog. Clin. Biol. Res.* **263,** 25–34
59. Nishikawa, M., Ikeda, H., Fukuda, T., Suzuki, S., and Okubo, T. (1990) Acute exposure to cigarette smoke induces airway hyper-responsiveness without airway inflammation in guinea pigs. Dose-response characteristics. *Am. Rev. Respir. Dis.* **142,** 177–183
60. Morrison, D., Rahman, I., Lannan, S., and MacNee, W. (1999) Epithelial permeability, inflammation, and oxidant stress in the air spaces of smokers. *Am. J. Respir. Crit. Care Med.* **159,** 473–479
61. Aggarwal, A. N., Gupta, D., Sharma, C. P., and Jindal, S. K. (2004) Effect of household exposure to environmental tobacco smoke on airflow mechanics in asymptomatic healthy women. *Indian J. Med. Res.* **119,** 18–23
62. Schick, S., and Glantz, S. (2005) Philip Morris toxicological experiments with fresh sidestream smoke. More toxic than mainstream smoke. *Tob. Control* **14,** 396–404
63. Cereijido, M., Valdés, J., Shoshani, L., and Contreras, R. G. (1998) Role of tight junctions in establishing and maintaining cell polarity. *Annu. Rev. Physiol.* **60,** 161–177
64. Madara, J. L. (1998) Regulation of the movement of solutes across tight junctions. *Annu. Rev. Physiol.* **60,** 143–159
65. Petecchia, L., Sabatini, F., Varesio, L., Camoirano, A., Usai, C., Pezzolo, A., and Rossi, G. A. (2009) Bronchial airway epithelial cell damage following exposure to cigarette smoke includes disassembly of tight junction components mediated by the extracellular signal-regulated kinase 1/2 pathway. *Chest* **135,** 1502–1512
66. Reid, L. M., and Bhaskar, K. R. (1989) Macromolecular and lipid constituents of bronchial epithelial mucus. *Symp. Soc. Exp. Biol.* **43,** 201–219
67. Schmekel, B., Hörnblad, Y., Hvatum, M., Norlund, A. L., and Venge, P. (1995) Kinetic retrieval of eosinophil cationic protein, hyaluronan, secretory IgA, albumin, and urea during BAL in healthy subjects. *Chest* **108,** 62–67
68. Itano, N., Atsumi, F., Sawai, T., Yamada, Y., Miyaishi, O., Senga, T., Hamaguchi, M., and Kimata, K. (2002) Abnormal accumulation of hyaluronan matrix diminishes contact inhibition of cell growth and promotes cell migration. *Proc. Natl. Acad. Sci. U.S.A.* **99,** 3609–3614
69. Maytin, E. V., Chung, H. H., and Seetharaman, V. M. (2004) Hyaluronan participates in the epidermal response to disruption of the permeability barrier *in vivo*. *Am. J. Pathol.* **165,** 1331–1341
70. Takahashi, Y., Li, L., Kamiryo, M., Asteriou, T., Moustakas, A., Yamashita, H., and Heldin, P. (2005) Hyaluronan fragments induce endothelial cell differentiation in a CD44- and CXCL1/GRO1-dependent manner. *J. Biol. Chem.* **280,** 24195–24204
71. Pienimaki, J. P., Rilla, K., Fulop, C., Sironen, R. K., Karvinen, S., Pasonen, S., Lammi, M. J., Tammi, R., Hascall, V. C., and Tammi, M. I. (2001) Epidermal growth factor activates hyaluronan synthase 2 in epidermal keratinocytes and increases pericellular and intracellular hyaluronan. *J. Biol. Chem.* **276,** 20428–20435
72. Rodgers, L. S., Lalani, S., Hardy, K. M., Xiang, X., Broka, D., Antin, P. B., and Camenisch, T. D. (2006) Depolymerized hyaluronan induces vascular endothelial growth factor, a negative regulator of developmental epithelial-to-mesenchymal transformation. *Circ. Res.* **99,** 583–589
73. Xu, Y., and Yu, Q. (2003) E-cadherin negatively regulates CD44-hyaluronan interaction and CD44-mediated tumor invasion and branching morphogenesis. *J. Biol. Chem.* **278,** 8661–8668
74. Zoltan-Jones, A., Huang, L., Ghatak, S., and Toole, B. P. (2003) Elevated hyaluronan production induces mesenchymal and transformed properties in epithelial cells. *J. Biol. Chem.* **278,** 45801–45810
75. Cywes, C., and Wessels, M. R. (2001) Group A Streptococcus tissue invasion by CD44-mediated cell signaling. *Nature* **414,** 648–652
76. Sköld, C. M., Blaschke, E., and Eklund, A. (1996) Transient increases in albumin and hyaluronan in bronchoalveolar lavage fluid after quitting smoking. Possible signs of reparative mechanisms. *Respir. Med.* **90,** 523–529
77. Jiang, D., Liang, J., and Noble, P. W. (2007) Hyaluronan in tissue injury and repair. *Annu. Rev. Cell Dev. Biol.* **23,** 435–461
78. Stern, R., Asari, A. A., and Sugahara, K. N. (2006) Hyaluronan fragments. An information-rich system. *Eur. J. Cell Biol.* **85,** 699–715
79. Olivera, D., Knall, C., Boggs, S., and Seagrave, J. (2010) Cytoskeletal modulation and tyrosine phosphorylation of tight junction proteins are associated with mainstream cigarette smoke-induced permeability of airway epithelium. *Exp. Toxicol. Pathol.* **62,** 133–143
80. Olivera, D. S., Boggs, S. E., Beenhouwer, C., Aden, J., and Knall, C. (2007) Cellular mechanisms of mainstream cigarette smoke-induced lung epithelial tight junction permeability changes *in vitro*. *Inhal. Toxicol.* **19,** 13–22
81. Bono, P., Cordero, E., Johnson, K., Borowsky, M., Ramesh, V., Jacks, T., and Hynes, R. O. (2005) Layilin, a cell surface hyaluronan receptor, interacts with merlin and radixin. *Exp. Cell Res.* **308,** 177–187
82. Peroni, D. G., Djukanović, R., Bradding, P., Feather, I. H., Montefort, S., Howarth, P. H., Jones, D. B., and Holgate, S. T. (1996) Expression of CD44 and integrins in bronchial mucosa of normal and mildly asthmatic subjects. *Eur. Respir. J.* **9,** 2236–2242
83. Wimmel, A., Kogan, E., Ramaswamy, A., and Schuermann, M. (2001) Variant expression of CD44 in pre-neoplastic lesions of the lung. *Cancer* **92,** 1231–1236
84. Wimmel, A., Schilli, M., Kaiser, U., Havemann, K., Ramaswamy, A., Branscheid, D., Kogan, E., and Schuermann, M. (1997) Preferential histiotypic expression of CD44-isoforms in human lung cancer. *Lung Cancer* **16,** 151–172
85. Kasper, M., Günthert, U., Dall, P., Kayser, K., Schuh, D., Haroske, G., and Müller, M. (1995) Distinct expression patterns of CD44 isoforms during human lung development and in pulmonary fibrosis. *Am. J. Respir. Cell Mol. Biol.* **13,** 648–656
86. Lackie, P. M., Baker, J. E., Günthert, U., and Holgate, S. T. (1997) Expression of CD44 isoforms is increased in the airway epithelium of asthmatic subjects. *Am. J. Respir. Cell Mol. Biol.* **16,** 14–22
87. Wang, M. H., Wang, D., and Chen, Y. Q. (2003) Oncogenic and invasive potentials of human macrophage-stimulating protein receptor, the RON receptor tyrosine kinase. *Carcinogenesis* **24,** 1291–1300
88. Monzón, M. E., Manzanares, D., Schmid, N., Casalino-Matsuda, S. M., and Forteza, R. M. (2008) Hyaluronidase expression and activity is regulated by pro-inflammatory cytokines in human airway epithelial cells. *Am. J. Respir. Cell Mol. Biol.* **39,** 289–295